ARTICLE 17

Excited electron: SPA IV: Silpovgar IV with Piepflui. Excess relativistic: influence in LAN and SPA.

Javier Silvestre www.eeatom.blogspot.com

ABSTRACT

This is 17th article of 24 dedicated to atomic model based on Victoria equation (Articles index is at end). Relation of Silva de Peral y Alameda (SPA) is studied in [5,7] and refers to excited states and provides linearity between specific energy relationship and LAN of Serelles Secondary Line [2,4] that allows creation of said secondary line obtained from Torrebotana Central Line [1].

[6] and [7] are first and second and this is third and last of three articles that make up a unit. First part of this article concludes Silpovgar study on n_ss→ns with Mc Flui transform for Silpovgar III and part two of Silpovgar I. Second part is centred on other jumps behaviour that lead to confluence of Silpovgar IV. Third part closes with 5) Other electronic jumps and emphasizes in Silpovgar IV: on the one hand at X→np jump location and on the other with Piepflui or Constant spacing. Finally, $1s^2$→1sns (Term=^{1}S and J=0) brings two main points: Primitive energetic correlation of Silva de Peral y Alameda (SPA PEC) and First application of Relativistic effects.

KEYWORDS

Relation of Silva de Peral y Alameda, SPA relation, Silpovgar IV, Mc Flui transform, Piepflui, FEC, AFEC, PEC, Tete-Vic equation, LAN, Excess relativistic, ER_o, ER_{dR}, Feliz Theory of E_o, Feliz Representation of E_o

INTRODUCTION

This is third and last of triple article initiated with Relation of Silva de Peral & Alameda II: jump from n_ss to ns [6] and continued with SPA III: Mc Flui transform for Silpovgar III and Silpovgar IV[7] . Scheme, formulas and figures numbering is unique for three articles giving greater unity sense. Abbreviations Table is at end article. Scheme is as follows:

SPA IV: Silpovgar IV with Piepflui. Excess Relativistic: influence in LAN and SPA

- 5) Other electronic jumps (Continuation)
  - C) n_s(p or s)→np (Term=$^2P^0$ and J=3/2 (or 1/2)) with FEC adapted
  - In general, this point is applied to any $n_s(p^y$ or $s^x)$→ $n_s(p^{y-1}$ or $s^{x-1})$np
- P58 $n_s(p^y$ or $s^x)$→ $n_s(p^{y-1}$ or $s^{x-1})$np jump location in Silpovgar IV
- P59 Piepflui: Constant spacing for Silpovgar IV
  - D) $1s^2$→1sns (Term=^{1}S and J=0)
    - P60 Primitive energetic correlation of Silva de Peral y Alameda (SPA PEC)
- 6) Relativistic effects: First application made on D) $1s^2$→1sns (Term=^{1}S and J=0)
  - P61 IE Excess Relativistic in SPA PEC

P62 Feliz Theory of E_o vision from electron as moves away.
P63 ER_o interatomic behaviour
P64 Feliz representation of E_o vision from electron as moves away.

C) n_s(p or s)→np (Term=$^2P^0$ and J=3/2 (or 1/2)) with FEC adapted
In general, this point is applied to any $n_s(p^y$ or $s^x) \rightarrow n_s(p^{y-1}$ or $s^{x-1})np$

Jumps may need intermediate excited state which is included in FEC conforming adaptation FEC (P57 FEC adapted or AFEC). This intermediate excited state for $n_sp \rightarrow np$ and, in general, for all jump $n_sp^y \rightarrow n_sp^{(y-1)}ns$ is given by (18) and in the case of $n_ss^x \rightarrow n_sx^{(x-1)}np$ by (19):

$$(18)\ n_sp^y \rightarrow n_sp^{(y-1)}(n-1)p \rightarrow n_sp^{(y-1)}np$$

$$(19)\ n_ss^x \rightarrow n_sx^{(x-1)}(n-1)p \rightarrow n_ss^{(x-1)}np$$

Initial state → intermediate excited state → excited state

As indicated in P57 FEC adapted or AFEC, intermediate excited state which is included in FEC conforming adaptation FEC (20). (20) is transformed into (1) when intermediate excited state does not exist.

$$(20)\mathrm{AFEC}\left[n_s(p^y \text{ or } s^x) \rightarrow n_s(p^{y-1} \text{ or } s^{x-1})np\right] = \frac{-\left(IE + E_{k\ of\ (n-1)p}\right)}{E_{k\ of\ np} - E_{k\ of\ (n-1)p}}$$

Silpovgar IV compliance is demonstrated with several isoelectronic series examples with sufficient and accurate data in [7]. These isoelectronic series are in **Table 16.** These examples are represented in **Figure 17** and also converge at the same Piepflui point (FEC=2.75). $2p^*$, $3p^*$ and $4p^*$ are other isoelectronic series with start state in $2p^y$ $3p^y$ and $4p^y$ respectively and have not been individually included. Two np→ns jumps are also included because of their relevance in P58. These two isoelectronic series are Al 3p→5s and B 2p→5s and are indicated as Al-5s and B-5s respectively in Figure 17 and Table 16.

Figure 17 - SPA and Silpovgar IV. Isoelectronic series X→5p

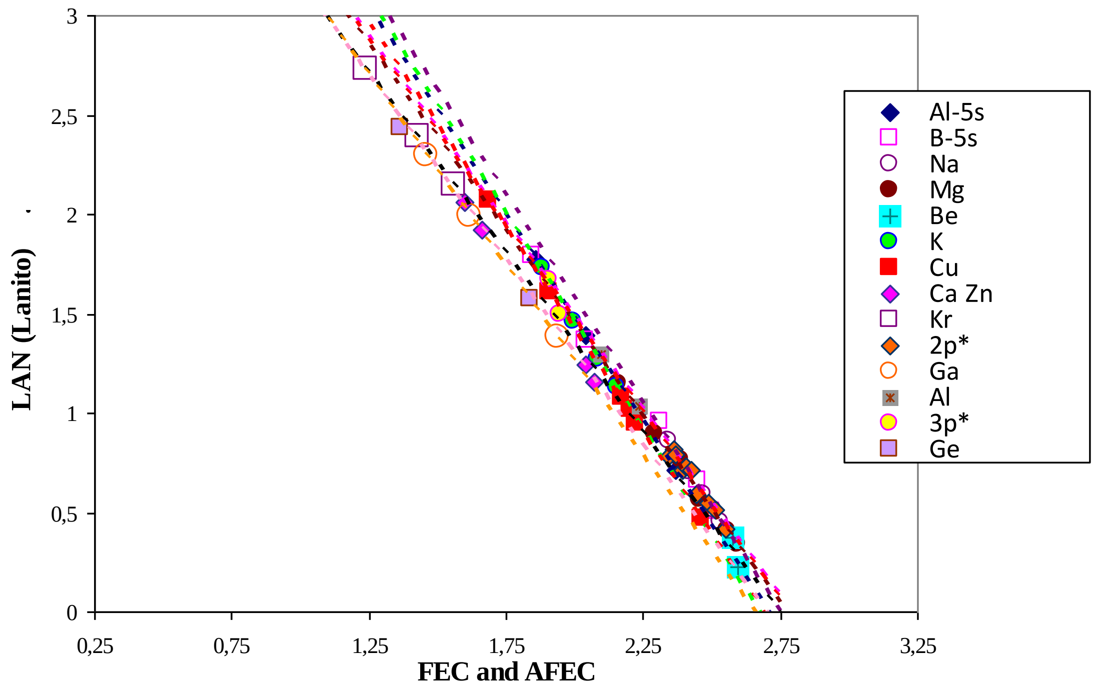

Table 16 - X→5p electron jump: isoelectronic series examples that meet Piepflui with AFEC (Isoelectronic series of Al (3p→5s) and B (2p→5s) are also included)

Isoelectronic series	Initial state	Intermediate (n=4) and excited state (n=5)	Atoms
Al (Al-5s)	3p ($^2P^0$ 1/2)	[Ne]$3s^2$ns ^2S 1/2	Al I, Si II, S IV and K VII
B (B-5s)	2p ($^2P^0$ 1/2)	[He]$2s^2$ns ^2S 1/2	B I, C II and N III
Na	3s (^2S 1/2)	[Ne]np ($^2P^0$ 3/2)	[Na I, P V]
Mg	$3s^2$ (^1S 0)	[Ne]3snp ($^3P^0$ 1)	[Mg I, S V] and Ar VII
Be	$2s^2$ (^1S 0)	[He]2snp ($^3P^0$ 1)	Be I and B II
K	4s (^2S 1/2)	[Ar]np ($^2P^0$ 3/2)	[K I, Ti IV]
Cu	4s (^2S 1/2)	[Ar]$3d^{10}$np ($^2P^0$ 3/2)	Cu I, Ga III, Kr VIII, Rb IX, Sr X, Xe XXVI
Ca Zn	$4s^2$ (^1S 0)	4snp ($^3P^0$ 1)	Ca I, Ga II, Kr VII, Rb VIII
Kr	$4p^6$ (^1S 0)	[Ar]$3d^{10}4s^24p^5$($^2P^0$ 3/2)np ^{2}[1/2]1	[Kr I, Sr III]
2p* Ne	$2p^6$ (^1S 0)	[He]$2s^22p^5$($^2P^0$ 3/2)np ^{2}[3/2]2	Ne I
2p* C	$2p^2$ (^3P 0)	[He]$2s^2$2pnp (^1S 0)	C I
		[He]$2s^2$2pnp (^1P 1)	C I

	N	$2p^3$ ($^4S^0$ 3/2)	[He]$2s^2 2p^2 np$ ($^2S^0$ 1/2)	N I and O II
			[He]$2s^2 2p^2 np$ ($^4P^0$ 5/2)	N I and O II
	O	$2p^4$ (^3P 2)	[He]$2s^2 2p^3$($^4S^0$)np (^5P 1)	O I and Ne III
			[He]$2s^2 2p^3$($^4S^0$)np (^3P 0)	O I
Ga		4p ($^2P^0$ 1/2)	[Ar]$3d^{10} 4s^2 np$ $^2P^0$ 3/2	Ga I, Ge II and Kr VI
Al		3p ($^2P^0$ 1/2)	[Ne]$3s^2 np$ $^2P^0$ 3/2	Al I and Si II
3p*	Si	$3p^2$ (^3P 0)	[Ne]$3s^2 3pnp$ (^1P 1)	Si I
	Ar	$3p^6$ (^1S 0)	[Ne]$3s^2 3p^5$($^2P^0$ 3/2)np ^{2}[3/2]2	Ar I
Ge		$4p^2$ (^3P 0)	[Ar] $3d^{10} 4s^2 4pnp$ (^1P 1)	Ge I and Kr V

P58 $n_s(p^y$ or $s^x) \rightarrow n_s(p^{y-1}$ or $s^{x-1})np$ jump location in Silpovgar IV

P58 is $n_s(p^y$ or $s^x) \rightarrow n_s(p^{y-1}$ or $s^{x-1})np$ jump location in small space of AFEC vs LAN representation and corresponding to np→ns area.

Figure 18 - SPA and Silpovgar IV. Isoelectronic series X→5p. LIMITS

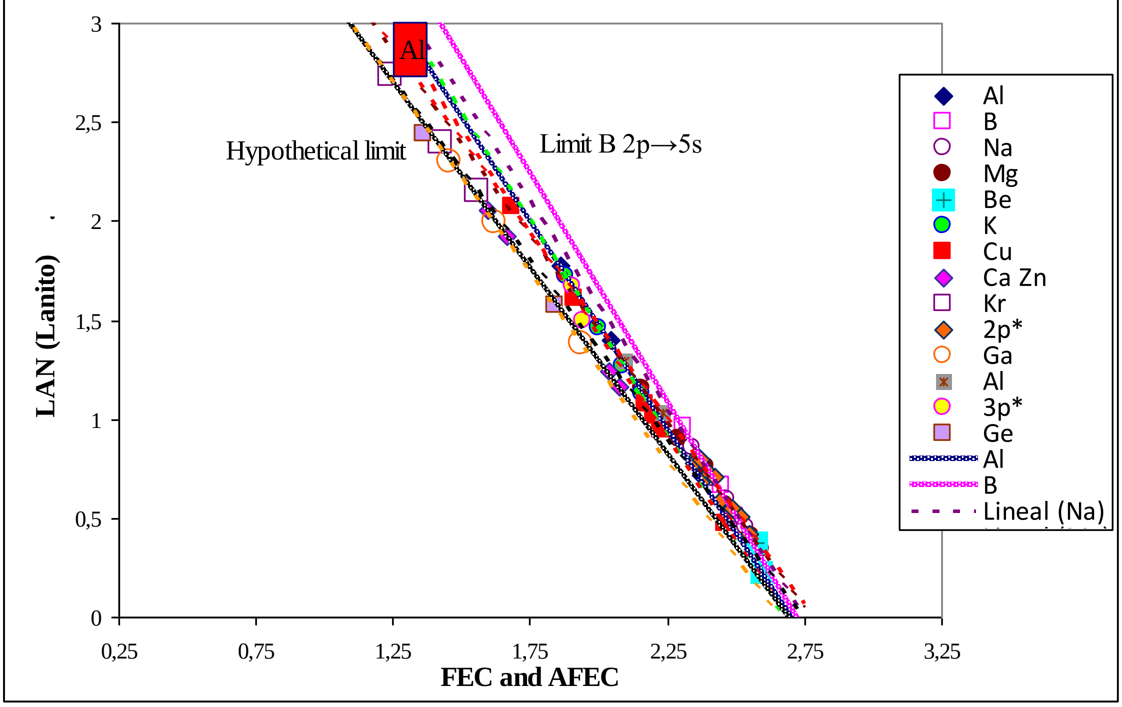

There are two particular relevant details in Figure 17:

* Isoelectronic series are more concentrated in X→5p (Figure 17) than in X→5s (Figure 16). Both axes have been maintained for better comparison between two figures.

* Isoelectronic series concentration zone is located between 3p→5s (Al series) that exerts of centre and two theorists limits equidistant to centre (**Figure 18**):

- 2p→5s (B isoelectronic series)
- Hypothetical limit.

P59 Piepflui: Constant spacing for Silpovgar IV

Piepflui or convergence point in Silpovgar IV representation (AFEC vs. LAN) occurs when LAN=0 and its AFEC value has constant spacing (21). Most of jumps present Silva de Peral y Alameda linearity with AFEC and few exceptions belong to first excited state. n is destiny n or excited state n:

$$(21)\text{Piepflui} = \frac{1}{4} + \frac{n}{2} = \frac{1+2n}{4}$$

P59 Piepflui application examples:

P59.A) $1s^2$→ns (Term=^{3}S and J=1)

First excited state (1s2s) presents problem to apply (17) since 1p does not exist. Regression, either lineal or polynomial of degree 2 with better R^2→1, tends to 1+1/3 instead of to 1+1/4 (21). Other jumps comply with P59 Piepflui as is appreciable in **Figure 19** where atoms from He I to Na X are represented.

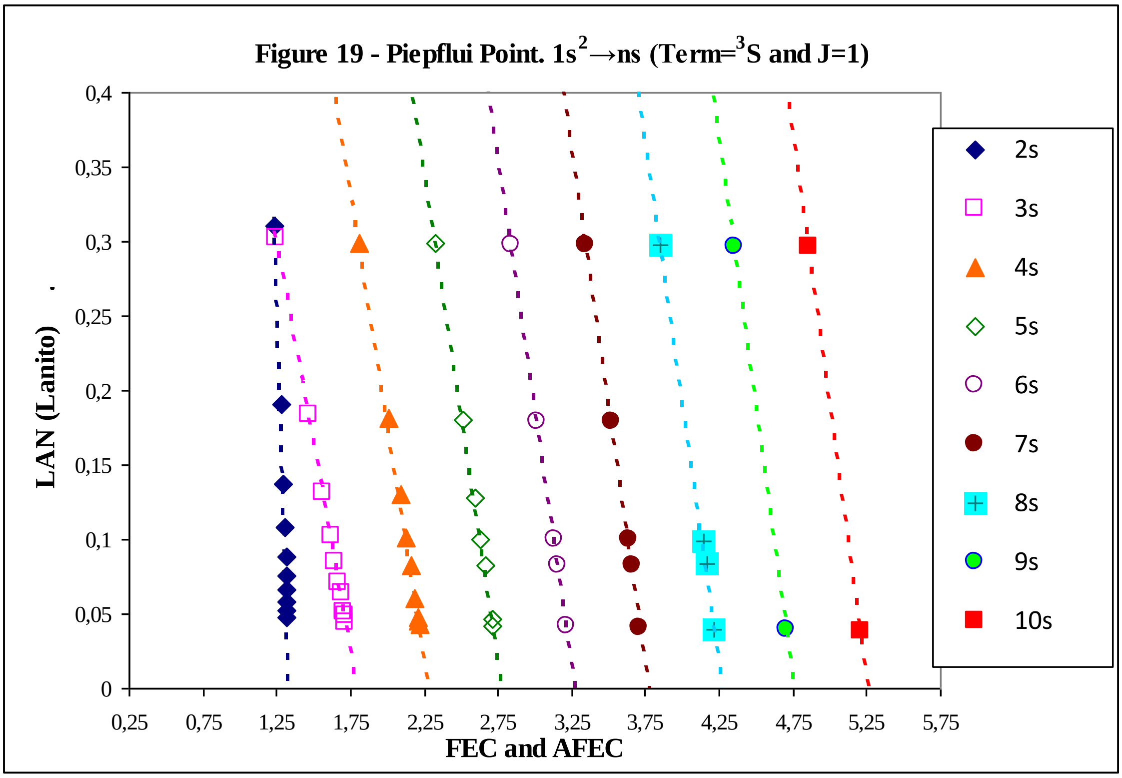

This intermediate excited state in general case of $n_s s^x$→ $n_s x^{(x-1)}$np is given by (19), but Term and J should be specified when there is more than one option. In this case, mechanism is (22). 1s(n-1)p (Term=$^3P^0$ and J=2) has been represented and J can be 0, 1 and 2:

(22) $1s^2 \rightarrow$ 1s(n-1)p (Term=$^3P^0$ and J=0,1,2) $\rightarrow$ 1sns (Term=^3S and J=1)

Slight deviations from P59 Piepflui (21) are reduced when z_s increases (**Figure 20**). This aspect with its possible extrapolation to other electron jumps should be studied with Relation of Riquelme de Gozy curvature developed in next article. Several alternate atoms have been selected for Figure 20: S XV, Sc XX, Ti XXI, Co XXVI, Ga XXX and Kr XXXV.

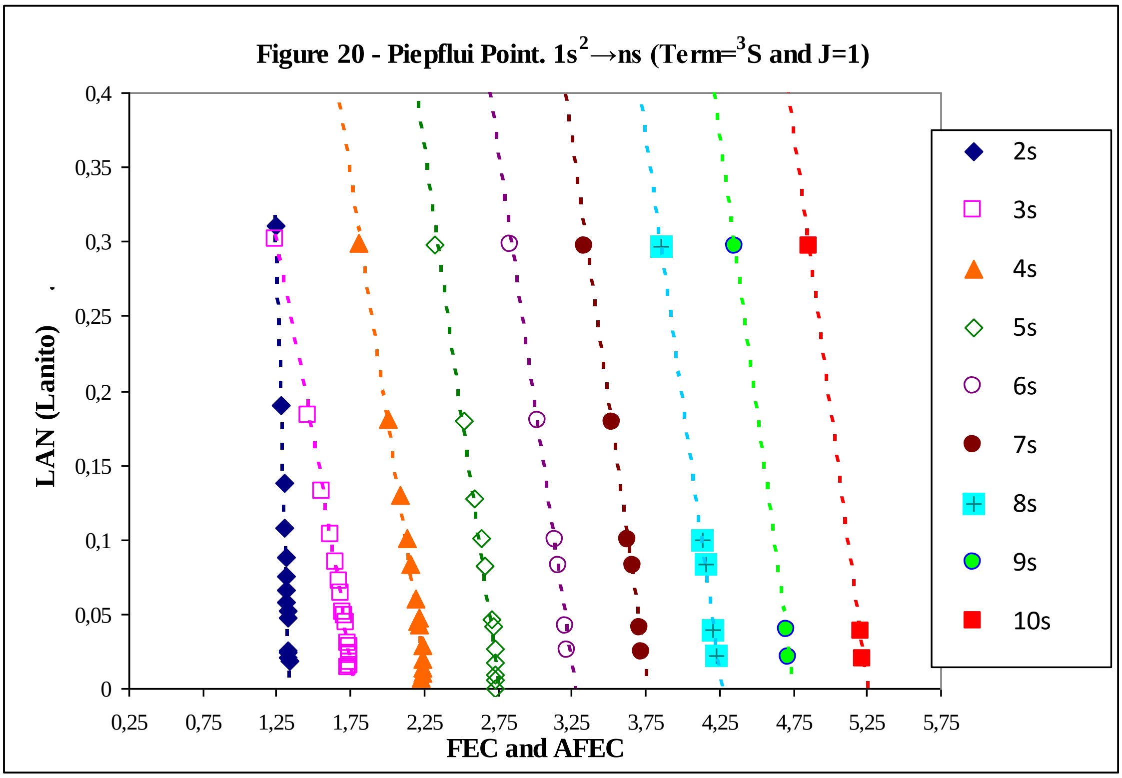

P59.B) Several jumps

Figure 21 has been realized considering mechanisms (14), (16), (18) and (19) and formulas (15), (17) and (20). Jump legend indicates: isoelectronic series – destiny n and s or p destiny. For example, "Al-5p" means Aluminium isoelectronic series and 5p destiny (3p→5p). In Figure 21, Piepflui (21) has also been included in regressions calculation for first time. Figure 21 is focused on destiny n equal to 3, 4 or 5.

P59 Piepflui: Constant spacing for Silpovgar IV begins with: "Most of jumps present Silva de Peral y Alameda linearity with AFEC and few exceptions belong to first excited state." First excited state in $n_sp^6 \rightarrow n_sp^5(n_s+1)s$ is only exception of Figure 21 and therefore are legends: Ne-3s, Ar-4s and Kr-5s and their LAN vs. AFEC points are located following second-order polynomial regression.

Figure 22 is equivalent to Figure 21 but n destiny is the later ones: 6, 7 and 8. Piepflui protagonism is demonstrated in both figures.

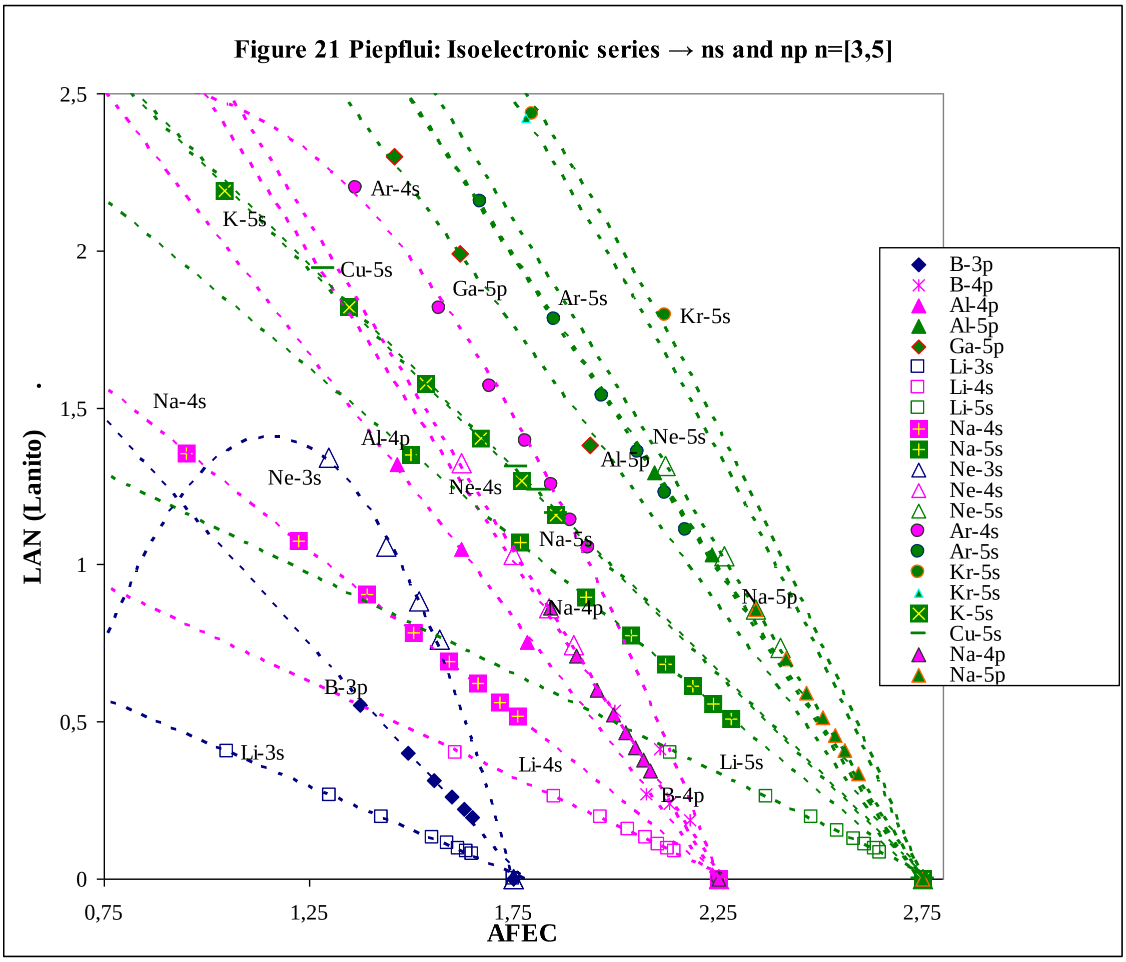

Figure 22 Piepflui: Isoelectronic series → ns and np n=[6,9]

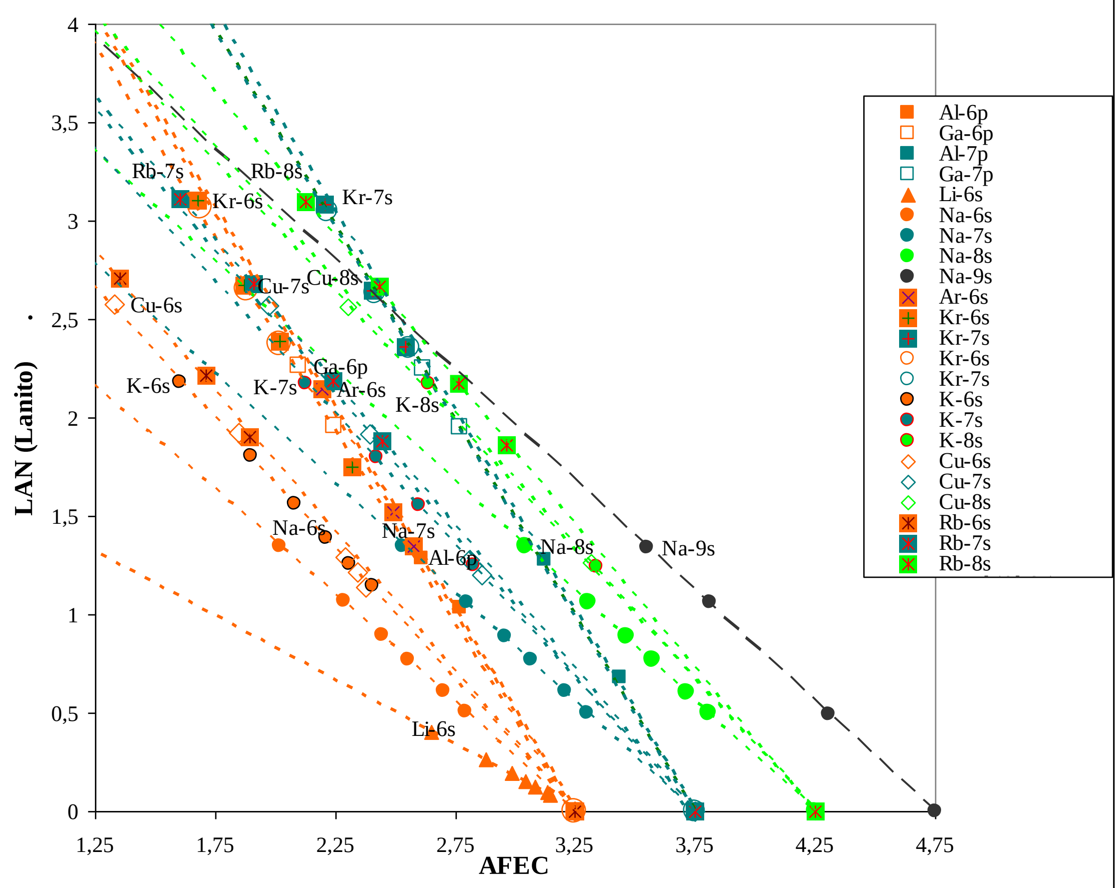

D) $1s^2 \rightarrow 1sns$ (Term=^1S and J=0)

$1s^2 \rightarrow 1sns$ (Term=^3S and J=1) and $n_Ss \rightarrow ns$ (Term=^2S and J=1/2) has been studied as example fulfilling Relation of Silva de Peral y Alameda (SPA relation) as well as Piepflui point (Figure 19 and 20) [5] and [6]. Another $1s^2 \rightarrow 1sns$ jump remains to be analyzed because there are two destination states (excited states) (**Table 17**). "Destiny state 1" maintains opposite spins as start state and is treated now. "Destiny state 1" is considered as "Primitive Jump" or "First Jump" because is the simplest jump of atom with more than one electron. "Destiny state 1" has particular energetic correlation (EC) as is introduced in [5]. "Primitive Jump" or "First Jump" is governed by P60 Primitive energetic correlation of Silva de Peral y Alameda (SPA PEC).

Table 17 - Start and destiniy states for $1s^2 \rightarrow 1sns$

State	Start state	Destiny state 1	Destiny state 2
Configuration	$1s^2$ (^1S and 0)	1sns (^1S and 0)	1sns (^3S and 1)
Spin	↑↓	↑ ↓	↑ ↑

P60 Primitive energetic correlation of Silva de Peral y Alameda (SPA PEC)

SPA PEC is quotient between 1s ionization energy (E_o) and $1s^2$ ionization energy (IE) (23). SPA PEC is jump energy independent and therefore is outstanding difference with respect to FEC (Fundamental energetic correlation) that is equal to quotient between ionization energy of excitable electron (IE) and excited state energy (E_k) (24).

$$(23)PEC = \frac{E_o}{IE}$$

$$(24)FEC = \frac{/IE/}{E_k} = \frac{-IE}{E_k}$$

LAN vs. FEC and PEC for $1s^2 \rightarrow 1s2s$ (Term=^1S and J=0) from He to Kr is represented in **Figure 23**. SPA relation of PEC (R^2=0.9991) is better than R^2=0.9956 of FEC. Important difference between both energetic correlations is different sense when z_S increases:

* FEC: $\uparrow z_S \rightarrow \uparrow$FEC and FEC$\rightarrow$Fluipoint
* PEC: $\uparrow z_S \rightarrow \downarrow$PEC and PEC$\rightarrow$1 (IE=$E_o$)

Figure 23 - SPA relation with FEC and PEC for $1s^2 \rightarrow 1s2s$ (Term=^1S J=0)

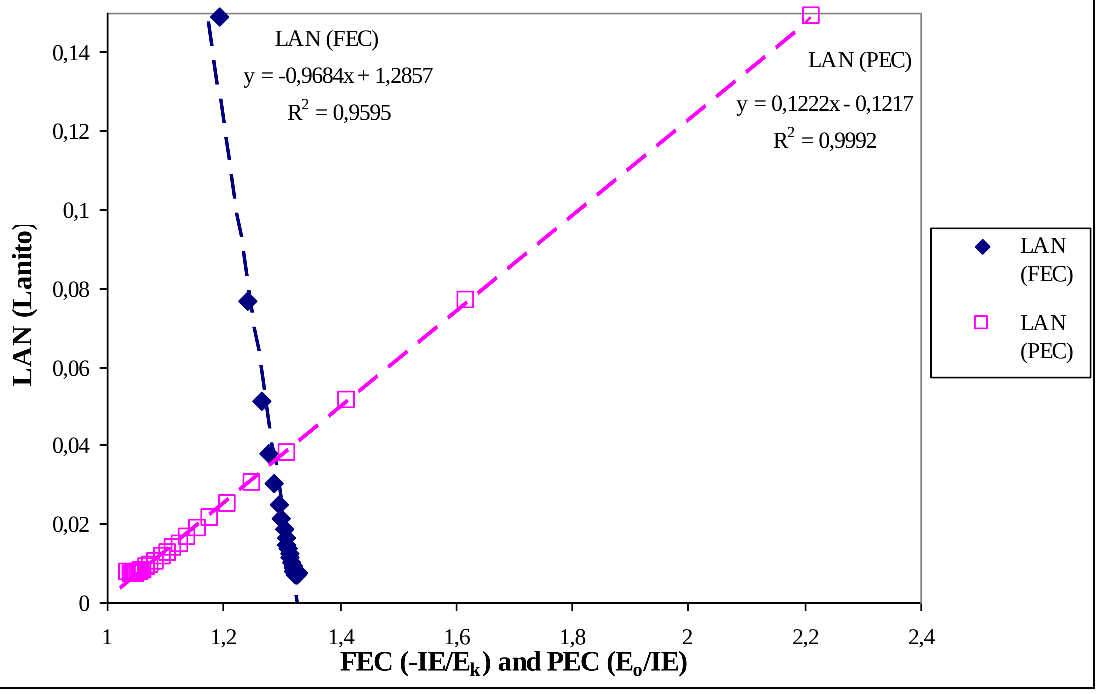

P61 IE Excess Relativistic in SPA PEC

PEC vs. LAN has slight curvature when Z is high (PEC→1) whose explanation must consider IE which is the most important change between $1s^2 \rightarrow 1s2s$ and another closely studied jump such as $1s^2 2s \rightarrow 1s^2 3s$:

$$/IE(1s^2)/ >> /IE(2s)/ \text{ for same } z_s \rightarrow 1s2s \text{ ER} >> 1s^2 3s \text{ ER}$$

and affects to greater extent LAN(1s2s) calculation.

Reversion to linearity is promoted through Excess Relativistic (ER) of $E_{dR}(1s2s)$ which is estimated from 1s ER. 1s ER defined as difference between theoric E_o (E_{oT}) and experimental E_o [7] (25):

$$(25)\ 1s\ ER = E_{oT} - E_o = -13.6056899\ eV * Z^2 - E_o$$

1s ER is obtained from Be to Si, [Be, Si], with E_o=[-217.718577, -2673.182] and ER=[0.0275382, 6.4667796] and second degree polynomial equation is (26):

$$(26)\ 1s\ ER\ [Be, Si] = 0{,}000000932\ E_o^2 + 0{,}000072416\ E_o + 0{,}000392871$$
$$R^2 = 1{,}000000$$

Same operation is performed from Si to Ge with E_o=[-2673.182, -14119.429] and ER=[6.4667796, 187.202542] and second degree polynomial equation is (27):

$$(27)\ 1s\ ER\ [Si, Ge] = 0{,}000000954\ E_o^2 + 0{,}000231027\ E_o + 0{,}300557746$$
$$R^2 = 1{,}000000$$

(25) and (27) are applied for calculation of 1s2s ER, i.e. for first excited state $1s^2 \rightarrow 1s2s$ (Term=^1S and J=0) from He to Kr represented in Figure 23. This 1s2s ER is included in reference destiny energy (E_{dR}) (**Table 18**).

Table 18 - $1s^2 \rightarrow 1s2s$ (Term=^1S and J=0) E_{dR} including ER			
Symbol	$E_{dR}(1s2s)$	ER $E_{dR}(1s2s)$	$E_{dR}(1s2s)$ with ER
N	-125,65171	0,0060	-125,6457
O	-170,44018	0,0151	-170,4251
F	-222,0069	0,0303	-221,9766
Ne	-280,47209	0,0534	-280,4187
Na	-345,789	0,0868	-345,7022
Mg	-417,9678	0,1329	-417,8349
Al	-497,0283	0,1946	-496,8337
Si	-582,981	0,2749	-582,7061
S	-775,6534	0,5049	-775,1485
Ar	-996,3648	0,8535	-995,5113
K	-1116,8178	1,0820	-1115,7358

Sc	-1379,4264	1,6739	-1377,7525
Ti	-1521,3015	2,0472	-1519,2543
V	-1670,28	2,4796	-1667,8004
Cr	-1826,3965	2,9770	-1823,4195
Mn	-1989,6779	3,5459	-1986,1320
Fe	-2160,1649	4,1930	-2155,9719
Co	-2337,8869	4,9251	-2332,9618
Ni	-2522,8839	5,7498	-2517,1341
Cu	-2715,1985	6,6748	-2708,5237
Ga	-3121,7706	8,8765	-3112,8941
Kr	-4269,834	16,7069	-4253,1271

PEC vs. LAN of Figure 23 is enlarged in curvature zone with **Figure 24** when curvature increase as PEC decreases is appreciated. In addition, LAN calculated with $E_{dR}(1s2s)$ including ER is represented as LAN*. Conclusion is that $E_{dR}(1s2s)$ including ER corrects LAN curvature and SPA PEC linearity is achieved.

Figure 24 - SPA with PEC including 1s2s ER (Term=^{1}S J=0)

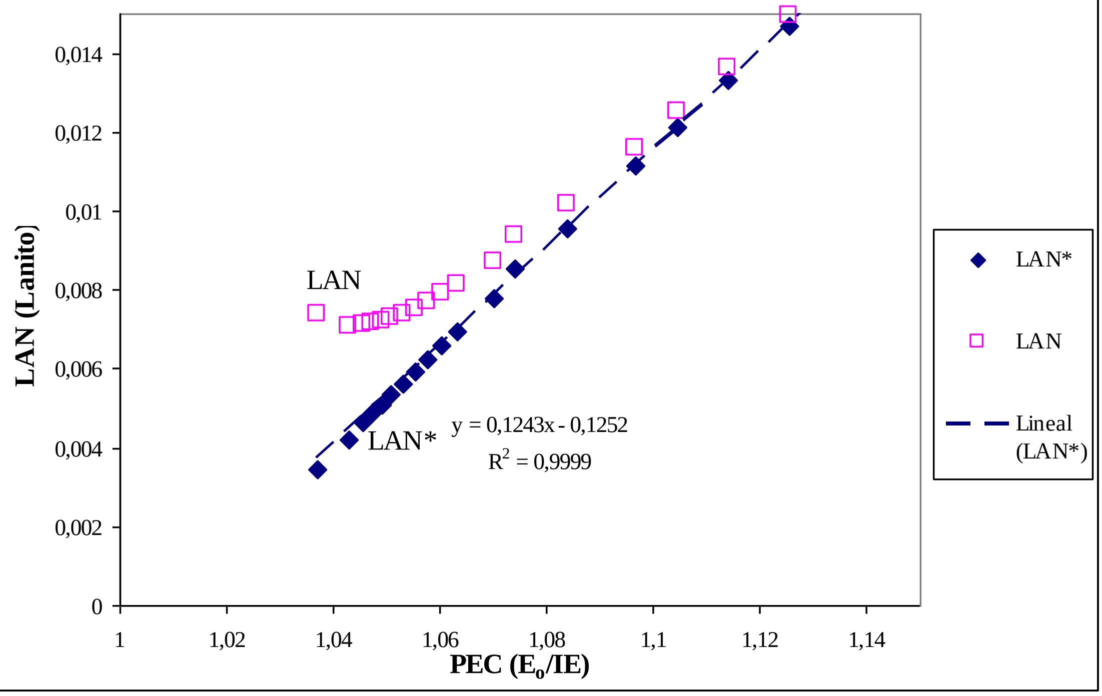

If only Excess Relativistic (ER) of $E_{dR}(1sns)$ effect exists, SPA PEC linearity without considering this effect must be accomplished gradually as n increases because $/E_{dR}/$ decreases and implies ER decreases.

$\uparrow$n $\rightarrow$ $/E_{dR}/\downarrow$ $\rightarrow$ ER $\downarrow$ $\rightarrow$ Effect on LAN $\downarrow$ $\rightarrow$ SPA PEC linearity without 1sns ER

This situation occurs, but more rapidly that predicted by such prior consideration. $1s^2 \rightarrow 1s3s$ (Term=^1S and J=0) without considering $E_{dR}(1s3s)$ ER is already located on SPA PEC linearity marked by LAN* 2s (LAN calculated with $E_{dR}(1s2s)$ including ER) in **Figure 25**. Figure 25 shows $1s^2 \rightarrow 1sns$ for n=[2,5] without ER as LAN ns and LAN calculated with $E_{dR}(1s2s)$ including ER is represented as LAN* 2s. In addition, $1s^2 \rightarrow 1sns$ with n>3 initiate deviation in reverse direction to that observed with $1s^2 \rightarrow 1s2s$. Conclusion is that there is another effect of inverse sense to E_{dR} ER: Excess Relativistic (ER) of E_o (1s) is source of this inverse effect because is included in LAN numerator while E_{dR} is in LAN denominator.

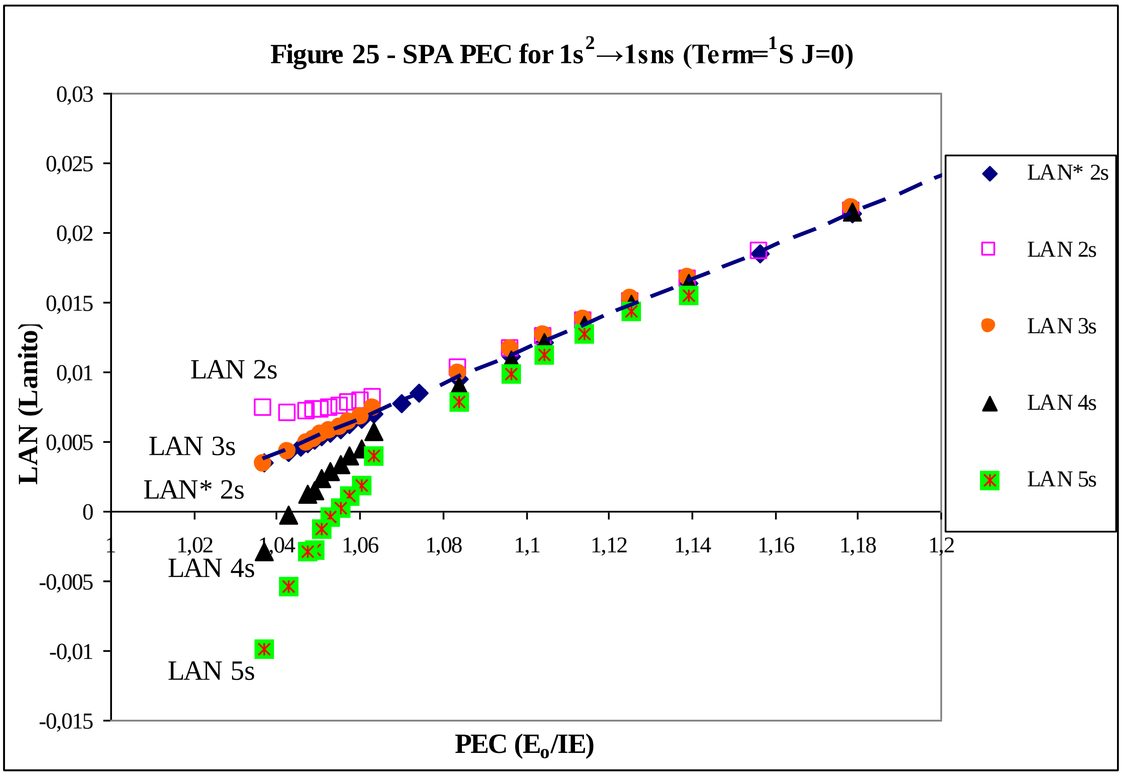

Relativistic (ER) of E_o (1s) is introduced with **LAN Feliz solution:**

P62 Feliz Theory of E_o vision from electron as moves away.

Linearity drift resolution in LAN vs. PEC (Figure 25), and in general for SPA relation, is obtained with progressive 1s ER (25) elimination in the vision of said 1s ER (25) by electron as it moves away.

Excess Relativistic (ER) of $E_{dR}(1sns)$ in $1s^2 \rightarrow 1sns$ (Term=^1S and J=0) with n=[3,5] is calculated using (26) because all jumps have $/E_{dR}/<2673.182$: Kr 1s3s has high energy with $/E_{dR}/=2113.987$ eV. LAN equation with ER incorporation in E_{dR} and E_o is given by (28) where ER consideration is indicated with *. E_{dR}^* and E_o^* are in (29) and (30). ER_{dR} is Excess Relativistic of reference destiny energy (E_{dR}) in general form to be indicated in (28) since when ER is of concrete jump is represented for example as "1s2s ER" or, more in detail if is not clear, as "1s2s (Term=^1S and J=0) ER". On the other hand, ER_o

is Excess Relativistic of 1s ionization energy (E_o) in the vision of said 1s ER (25) by electron as it moves away.

$$(28)\ -LAN^* \approx -LAN_R^* = \frac{(-E_o^*)^{1/2} z_s}{(-E_{dR}^*)^{1/2} z_o} - n = \frac{(-E_o - ER_o)^{1/2} z_s}{(-E_{dR} - ER_{dR})^{1/2} z_o} - n$$

$$(29)\ E_{dR}^* = E_{dR} + ER_{dR}$$

$$(30)\ E_o^* = E_o + ER_o$$

ER_o value (31) is obtained from (30) and (28):

$$(31) ER_o = -E_o - \left[\frac{(-LAN^* + n)(-E_{dR}^*)^{1/2} z_o}{z_s}\right]^2$$

LAN^* for $1s^2 \rightarrow 1sns$ (Term=^1S and J=0) is the same that LAN^* for $1s^2 \rightarrow 1s2s$ (Figure 24 as LAN^* and Figure 25 as LAN^* 2s) because PEC is jump energy (E_k) independent. FEC is E_k dependent and thus obtaining LAN^* differs. ER_o vs. E_o for $1s^2 \rightarrow 1sns$ (Term=^1S and J=0) with n=[3,5] is represented in **Figure 25** and shows curves without discontinuities where higher destiny n implies higher ER_o value. On the one hand, last comment, higher destiny n implies higher ER_o value, represents first contact with "P62 Feliz Theory of Eo vision from electron as moves away" because verifies progressive 1s ER (25) elimination.

Figure 26 - ER_o for $1s^2 \rightarrow 1sns$ (Term=^1S J=0) with (31)

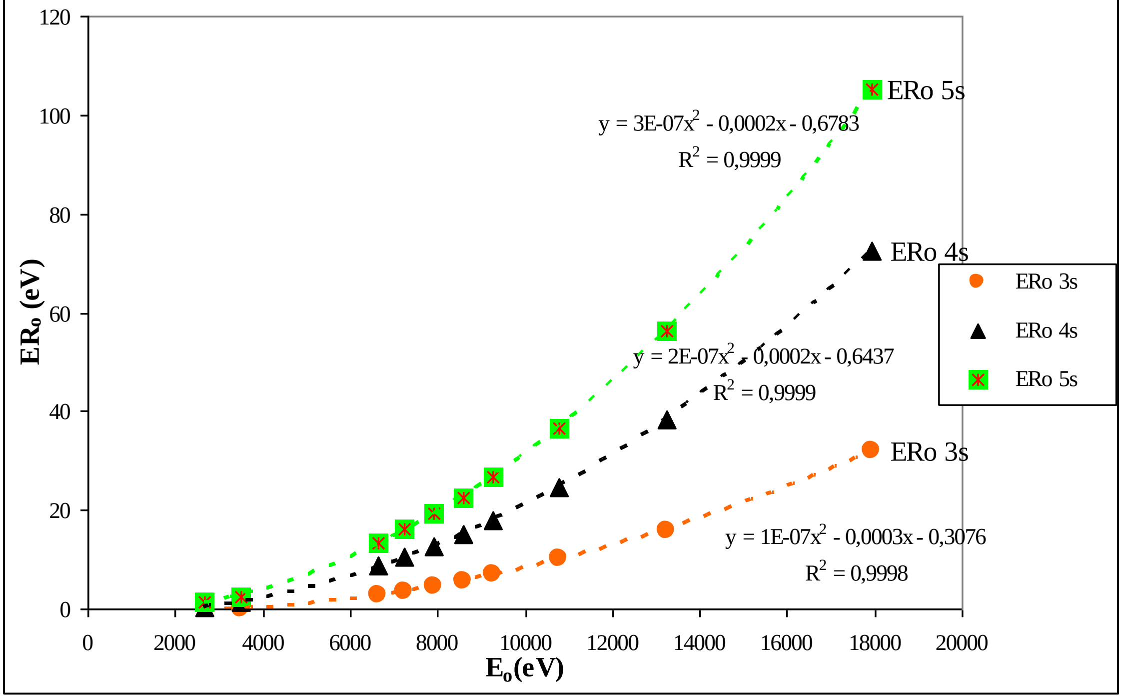

By other hand, P63 is intercalated in P62 explanation and develops ER_o interatomic behaviour where, among other conducts, ER_o vs. E_o curves must be studied.

P63 ER_o interatomic behaviour

ER_o, Excess Relativistic of 1s ionization energy (E_o) in the vision of said 1s ER (25) by electron as it moves away, show interatomic trends:

P63.A) ER_o vs. E_o has polynomial degree two polynomial regression (Figure 26) according selected n destiny which, considering curve between E_o and 1s ER, ends in P63.B

P63.B) ER_o vs. 1s ER (25) presents linearity as function of selected n destiny (**Figure 27**).

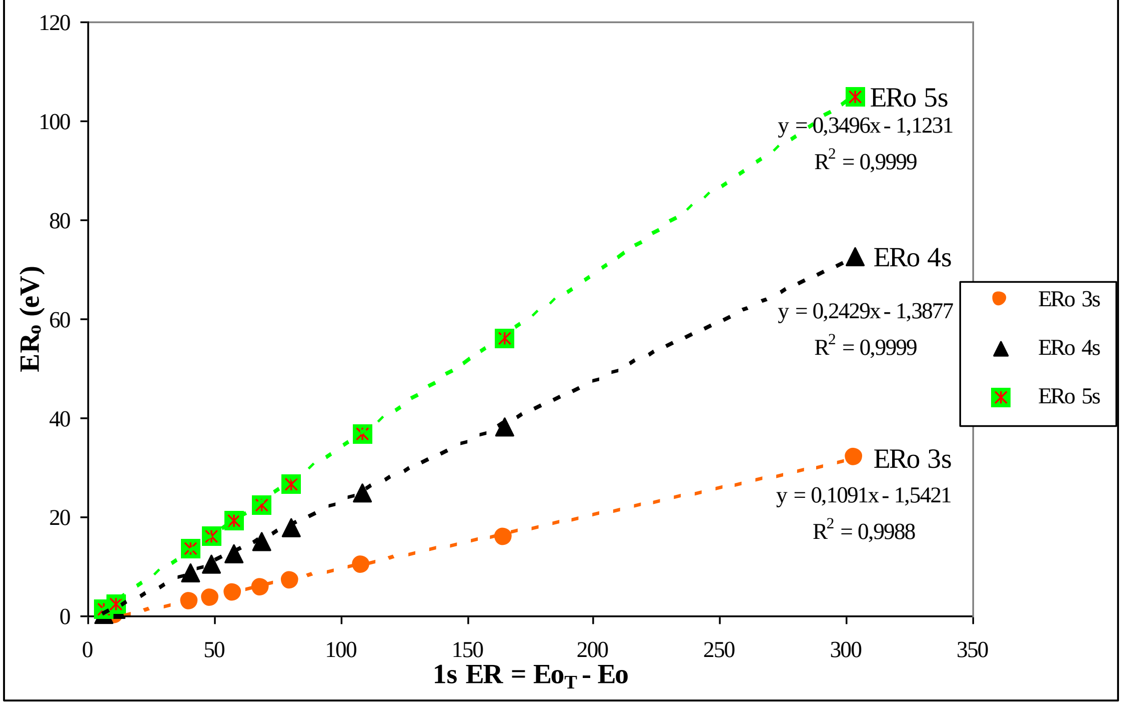

Figure 27 - SPA PEC for $1s^2 \rightarrow 1sns$ (Term=^1S J=0)

P62 continues with P64: representation of 1s ER (25) elimination in the view from electron as it moves away.

P64 Feliz representation of E_o vision from electron as moves away.

Feliz representation of E_o vision from electron as moves away is ER_o vs. $(-E_{dR})^{1/2}$ curve (32). Y-intercept must be equal to 1s ER (25) and therefore said 1s ER must be obtained from extrapolation of experimental data.

$$(32) ER_o \propto (-E_{dR})^{1/2}$$

Feliz representation is carried out with Kr $1s^2 \rightarrow 1sns$ (Term=^1S and J=0 and n=[2,4]) in **Figure 28**. Three jumps are adjusted to grade two polynomial regression (33). Y-intercept provided by equation is 295 eV and therefore very close to that expected:
1s ER= ER = E_{oT} - E_o = -13.6056899 eV * 36^2 - (-17936.208) = 303.23 eV. In addition, $ER_o \rightarrow 0$ when is Ed_R of 1s4s: $(-Ed_R)^{1/2}=(-4269.834 \text{ eV})^{1/2}=65.344 \text{ eV}^{1/2}$

$$(33) ER_o = a + b(-E_{dR})^{1/2} + c(-E_{dR})$$

In fact, inclusion of these two points, (0, 303.23) and (65.344, 0) provide R^2=0.9999 in grade two polynomial regression.

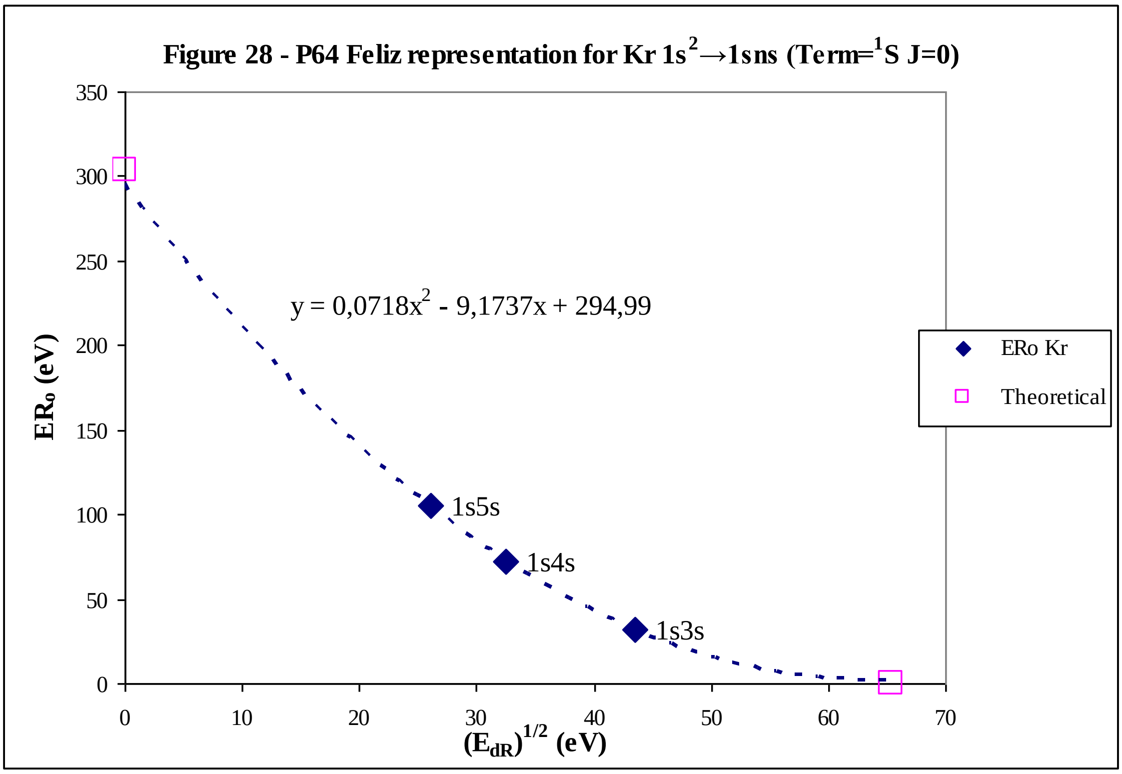

For example, Ga and Ti also give values with very good approximation with Y-intercept of 161 and 42 eV against 164 and 41 eV provided by (25).

In next article, corroboration of Feliz Theory of E_o vision from electron as moves away is done on other jumps as $[Ne]3s \rightarrow [Ne]ns$ that brings with important differences:

* /IE/ << /E_o/ implying that ER_{dR} is very small compared to ER_o and that difference increases as excitable electron is at higher n. ER_{dR} effect may be negligible especially at low z_s. Therefore, ER_o effect can be studied individually in some cases.

For example in Na, 1s ionization energy (E_o) is -1648,702 eV and similar to $1s^2$ IE=-1465.121 eV and this has been situation seen in P62, P63 and P64 because jump studied has been: $1s^2 \rightarrow 1sns$ (Term=^1S and J=0). In contrast, for example [He]2s IE=-299,864 eV or especially [Ne]3s IE=-5,13908 eV are much lower. ER_o >> ER_{dR} of 3s excited states.

* Electrons with low z_s usually have data at high n and, if also fulfil /IE/ << /E_o/, allow to investigate ER_o individually when $E_{dR} \to 0$ and consequently X-Axis of Feliz relativistic representation as well: $(E_{dR})^{1/2} \to 0$.

* ER_o vs. $(-E_{dR})^{1/2}$ section with medium-high n is approximated to line equation (34) from curve adjusted to grade two polynomial regression (33).

$$(34) ER_o \approx a + b(-E_{dR})^{1/2}$$

* LAN* (28) obtained from SPA relation in present article can also be given by Relation of Riquelme de Gozy [2,3] as seen in following article

Finally, simple study of ER_o and ER_{dr} effects on LAN is included in annex.

BIBLIOGRAPHY

[1] Javier Silvestre. Excited electrons by Torrebotana Central Line: Tete Vic Equation. Sent to: http://vixra.org/author/javier_silvestre

[2] Javier Silvestre. LAN plains for Tete Vic Equation. Sent to: http://vixra.org/author/javier_silvestre

[3] Javier Silvestre. Relation of Riquelme de Gozy: LAN lineality with energy of excited states. Sent to: http://vixra.org/author/javier_silvestre

[4] Javier Silvestre. Relation of Flui Piep de Garberí: LAN^{-1} and Ionization Energy. Sent to: http://vixra.org/author/javier_silvestre

[5] Javier Silvestre. Relation of Silva de Peral y Alameda: LAN interatomicity with energetic relation. Sent to: http://vixra.org/author/javier_silvestre

[6] Javier Silvestre. Relation of Silva de Peral & Alameda II: jump from n_ss to ns. Sent to: http://vixra.org/author/javier_silvestre

[7] Javier Silvestre. SPA III: Mc Flui transform for Silpovgar III and Silpovgar IV. Sent to: http://vixra.org/author/javier_silvestre

[8] Kramida, A., Ralchenko, Yu., Reader, J., and NIST ASD team (2014). NIST Atomic Spectra Database (ver. 5.2.) [Online]. Available: http://physics.nist.gov/asd [2016, May 30]. National Institute of Standards and Technology, Gaithersburg, MD

[9] Kramida, A., Ralchenko, Yu., Reader, J., and NIST ASD Team (2015). *NIST Atomic Spectra Database* (ver. 5.3), [Online]. Available: http://physics.nist.gov/asd [2016, May 18]. National Institute of Standards and Technology, Gaithersburg, MD.

Abbreviations Table Following Table indicates abbreviations used in this theory and its use in article in question is marked with X. 14, 15 and 16 are [5] [6] and [7] respectively. 17 is present article.					
Abbreviation	**14**	**15**	**16**	**17**	**Meaning**
AC	X				Actual Change
AFEC			X	X	FEC adapted
BES	X				Born Electronic System
E_{dR}	X	X		X	Reference destiny energy
E_{dR}^{*}				X	Reference destiny energy with ER_{dR}
E_k	X	X	X	X	Reference Jump energy
$E_{k\text{-}SPA}$	X				E_k from LAN-SPA equality
E_o	X	X		X	1s OES Ionization energy
E_o^{*}				X	1s OES Ionization energy with ER_o
E_{oT}				X	1s theoretical ionization energy
EC	X				Energetic correlation in SPA
ER				X	Excess Relativistic
ER_{dR}				X	Excess Relativistic of E_{dR}
ER_o				X	Excess Relativistic of 1s ionization energy (E_o)
FEC	X	X	X	X	Fundamental Energetic Correlation
FPG	X				Relation of Flui Piep de Garberí
IE	X	X	X	X	Ionization energy
LAN	X	X	X	X	Serelles Secondary Lines Factor
LAN_M				X	LAN with modification
LAN_R*				X	LAN with reference data and considering ER
LAN_R	X	X	X	X	LAN with reference data
LAN(P50)				X	Initial LAN value in ns to ns jump. LAN with IE
n	X	X	X	X	Principal quantum number
$n_{initial}$ or n_s	X	X	X	X	n of non-excited electron
OES	X				Origin Electronic System
PEC				X	Primitive energetic correlation of SPA
Piepflui				X	Constant spacing in Silpovgar IV
RC	X			X	Relative Change
RG	X	X			Relation of Riquelme de Gozy
SPA	X	X	X	X	Relation of Silva de Peral y Alameda
Z	X			X	Atomic Number
z_o	X	X			1s Origin charge according to P46
z_s	X	X		X	Start charge according to P46

ANNEX

Energetic changes effect on LAN

LAN has 2 energetic terms (1): Destiny energy of excitable electron that uses reference data [9] (E_{dR}) and born, initial or first electron energy (1s Energy) that is represented by E_o.

$$(1)\ \text{-}\ \text{LAN} \approx -\text{LAN}_R = \left(\frac{z_s{}^2 E_o}{z_o{}^2 E_{dR}}\right)^{1/2} - n = \left(\frac{z_s{}^2 E_o}{z_o{}^2 (E_K + IE)}\right)^{1/2} - n$$

(1) can be simplified in (2):

$$(2)\ \text{-}\ \text{LAN} \approx -\text{LAN}_R = \frac{(-E_o)^{1/2} z_s}{(-E_{dR})^{1/2} z_o} - n$$

Jump energy (E_k) [9] and Ionization energy [8] (IE) provides E_{dR} (3):

$$(3)\ E_{dR} = IE + E_k$$

The energy changes effect on LAN is also applicable on ground state of LAN for $n_s \rightarrow ns$ jump [3] (4):

$$(4)\ \text{-}\ \text{LAN(P50)} = -\text{LAN}_{ns \rightarrow ns} = \frac{(-E_o)^{1/2} z_s}{(-IE)^{1/2} z_o} - n_{initial}$$

Relative Change in percentage is given by (5) where LAN is calculation with (2) and LAN_M is LAN modified. LAN_M also represents actual LAN including Excess Relativistic (ER_o and ER_{dR}) represented by LAN^* (28) and for this reason (5) is thus formulated:

$$(5)\%RC_M(\text{LAN}) = \frac{\text{LAN} - \text{LAN}_M}{/\text{LAN}_M/} \bullet 100$$

(6) implies that energy destiny (E_d) is multiplied by factor F to provide E_{dM}. E_d is generally used and includes possibility of using E_{dR} and E_{dRM} in formulas.

$$(6) E_{dM} = E_d F$$

$\uparrow n \rightarrow \downarrow /E_d/ \rightarrow \downarrow /E_d$ - $E_{dM}/$ if F=constant (7). That is, Actual change in absolute value decreases as n increases when F=constant. Therefore, if Actual change in absolute value is constant or increases with n is because F also grows with n. This fact is related with two relativistic excess (ER_o and ER_{dr}).

$$(7)/E_d - E_{dM}/ = /E_d((1-F)/$$

LAN_M with E_{dM} and LAN with general E_d are in (8) and (9) respectively:

$$(8)\ \text{-}\ LAN_M = \frac{(-E_o)^{1/2} z_s}{(-E_{dM})^{1/2} z_o} - n$$

$$(9) - LAN = \frac{(-E_o)^{1/2} z_s}{(-E_d)^{1/2} z_o} - n$$

K_{LAN} is inserted into (8) and (9) to reach (11) by applying (5). $/LAN_M/$ is considered LAN because in most cases LAN is positive.

$$(10) K_{LAN} = \frac{(-E_o)^{1/2} z_s}{z_o}$$

$$(11) \%RC_M(LAN) = \frac{\frac{K_{LAN}}{(-FE_d)^{1/2}} - n - \frac{K_{LAN}}{(-E_d)^{1/2}} + n}{n - \frac{K_{LAN}}{(-FE_d)^{1/2}}} \bullet 100$$

Sum of terms allows transition from (11) to (12):

$$(12) \%RC_M(LAN) = \frac{\frac{K_{LAN} - F^{1/2} K_{LAN}}{(-FE_d)^{1/2}}}{\frac{-K_{LAN} + n(-FE_d)^{1/2}}{(-FE_d)^{1/2}}} \bullet 100$$

(13) is (12) with both denominators simplified:

$$(13) \%RC_M(LAN) = \frac{K_{LAN} - F^{1/2} K_{LAN}}{-K_{LAN} + n(-FE_d)^{1/2}} \bullet 100$$

(14) is (13) divided numerator and denominator by K_{LAN}:

$$(14) \%RC_M(LAN) = \frac{1 - F^{1/2}}{-1 + \frac{n(-FE_d)^{1/2}}{K_{LAN}}} \bullet 100$$

(15) is obtained from (9) and (10). (15) use causes (16) to be achieved from (14):

$$(15) n - LAN = \frac{K_{LAN}}{(-E_d)^{1/2}}$$

$$(16)\%RC_M(LAN) = \frac{1 - F^{1/2}}{-1 + \frac{nF^{1/2}}{n - LAN}} \bullet 100$$

(17) is (16), but considering LAN_M instead of LAN.

$$(17)\%RC_M(LAN) = \frac{1 - F^{1/2}}{-1 + \frac{n}{n - LAN_M}} \bullet 100$$

Three interesting situations are:

a) $\%RC_M(LAN) \rightarrow 100\%$ when $n \rightarrow \infty$ (18). (16) with $n \rightarrow \infty$ is transformed into (18) and $\%RC_M(LAN) \rightarrow 100\%$ because infinite terms are simplified each other and cause numerator and denominator to be identical:

$$(18)\%RC_M(LAN)_{n \rightarrow \infty} = \frac{1 - F^{1/2}}{-1 + \frac{\infty F^{1/2}}{\infty}} \bullet 100 = -100\%$$

b) $\%RC_M(LAN) \rightarrow 100\%$ when $LAN \rightarrow 0$ (19). (16) with $LAN \rightarrow 0$ is transformed into (19) and $\%RC_M(LAN) \rightarrow 100\%$ because LAN is negligible compared to n value and consequently situation is identical to previous one: numerator and denominator are identical:

$$(19)\%RC_M(LAN)_{LAN \rightarrow 0} = \frac{1 - F^{1/2}}{-1 + \frac{nF^{1/2}}{n}} \bullet 100 = -100\%$$

(18) and (19) occur because (5) is changed to (5.B.) when $n \rightarrow \infty$ or $LAN \rightarrow 0$:

$$(5.B.)\%RC_M(LAN)_{LAN \rightarrow 0} = \%RC_M(LAN)_{n \rightarrow \infty} = \frac{LAN - LAN_M}{/LAN_M/} \bullet 100 = \frac{-LAN_M}{/LAN_M/} \bullet 100 = -100\%$$

-100% has been indicated because LAN (and LAN_M) is mostly positive.

Therefore, both higher n and lower LAN imply an increase in deviation between both LAN. Lower LAN has been observed with z_s is increased [2,7]. All this leads to work with data from n↑ and LAN↓ (or z_s↑) is less accurate in SPA or RG relations. In addition, is necessary to add own experimental difficulties that present LAN value when n↑ and z_s↑.

c) $\%RC_M(LAN) \rightarrow \pm\infty$

This discontinuity is produced when (16) denominator is cancelled and is called discontinuity condition (33). n discontinuity condition (34) is obtained from (33) and is positive with physical sense if 0<F<1 since LAN is positive. This discontinuity causes that $\%RC_M$(LAN) vs. n curve to be different with 0<F<1 or F>1.

$$(33)\text{Discontinuity condition} = -1 + \frac{nF^{1/2}}{n - LAN} = 0$$

$$(34)\text{n discontinuity condition} = \frac{LAN}{1 - F^{1/2}}$$

a) and b) interesting situations discussed and high LAN sensibility to energetic variations can be verified with **Figure 29**. Figure 29 is $\%RC_M$(LAN) vs. log(n) curve with (16). X-axis is log(n) is for better visualization up to high n. LAN plain [2] is considered approximately constant. LAN value of third n destiny is selected so that approximation is more correct for high n destiny. These LAN value of third n destiny are as follows for indicated samples:

Li 2s→ns	0,40062309
Li 2s→np	0,04602786
Li 2s→nd	0,0008053
Na 3s→ns	1,34737865

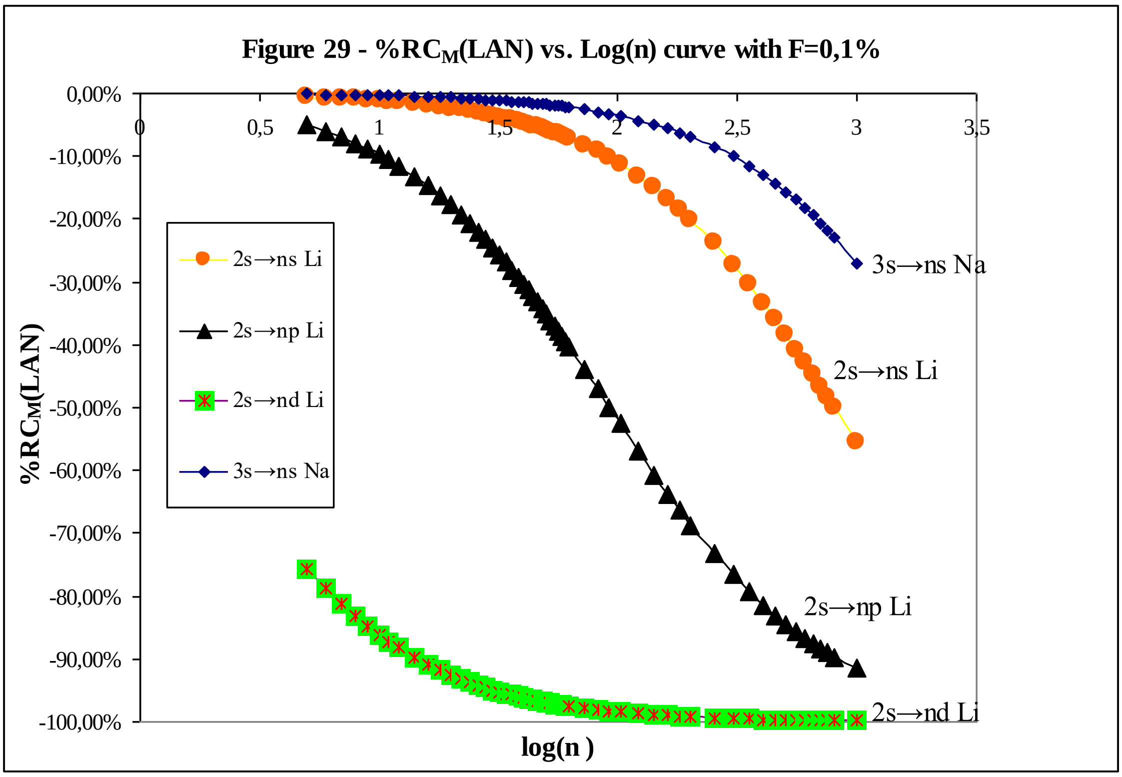

Figure 29 shows that both higher n and lower LAN imply an increase in deviation between both LAN (point a) and b) commented previously).

High sensitivity is also checked. (E_d) is multiplied by factor F to provide E_{dM} (6) and F selected is 1.001, i.e. variation of 0.1 %. LAN sensibility to energetic variations is corroborated because variations are much higher that 0.1 % (%RC_M(LAN)>>0.1%)

Even jumps with higher LAN (Li 2s→ns and Na 3s→ns) and lower n show %RC_M(LAN)>0.1%. (**Figure 30**). Figure 30 is %RC_M(LAN) vs. n curve with (16). X-axis is n and not log(n) to focus study at low n.

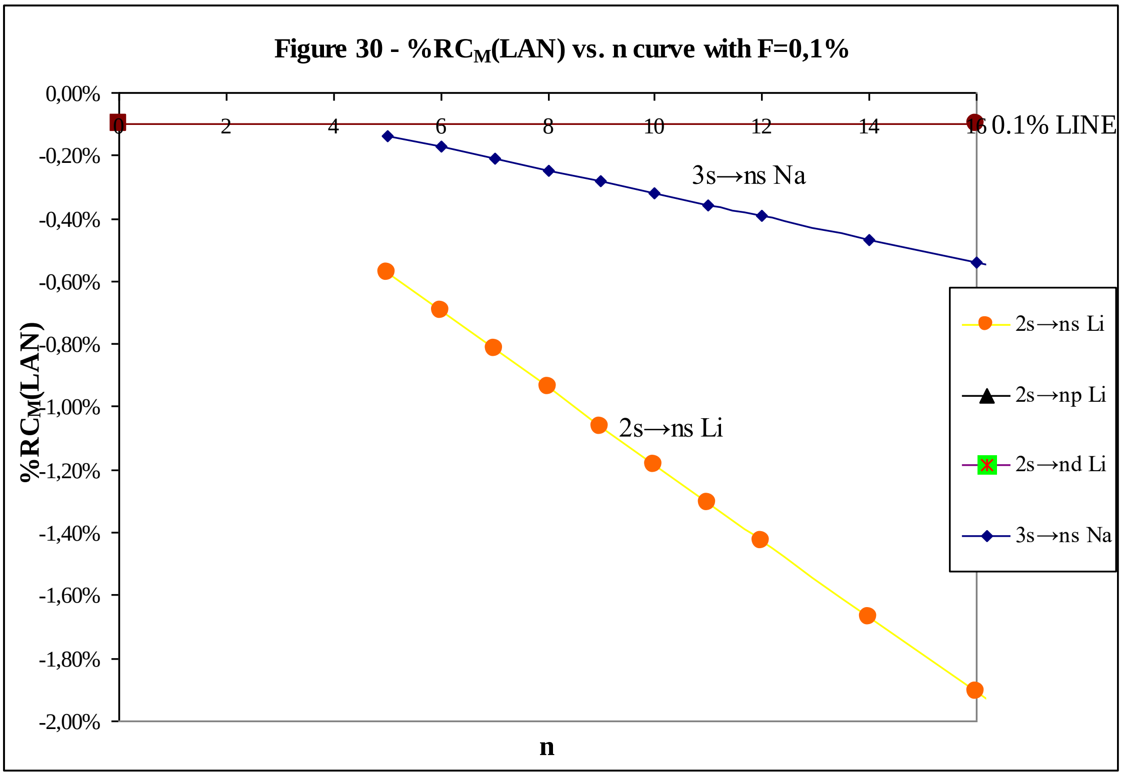

(20) and (6) are equalized as indicated in (21) if E_d deviation is x (20)

$$(20) E_{dM} = E_d + x$$

$$(21) E_d F = E_d + x$$

F (22) is obtained from (21) as x function and this F expression is included in (16) to arrive at (23):

$$(22) F = \frac{E_d + x}{E_d}$$

$$(23)\%RC_M(LAN) = \frac{1-\left(\frac{E_d+x}{E_d}\right)^{1/2}}{-1+\frac{n\left(\frac{E_d+x}{E_d}\right)^{1/2}}{n-LAN}} \bullet 100$$

(23) application with x=0.001 eV is performed on same jumps of Figures 29 and 30. x=0.001 eV because provides similar deviation as with F=1,001 for first jump shown. **Figure 31** represents $\%RC_M(LAN)$ vs. Log(n) curve with x=0,001 eV. Main conclusion is that $\%RC_M(LAN)$ increases faster with x=0,001 than with F=1,001 because E_d is decreasing and x=constant=0.001 eV is summed, and not multiplied as F, to E_d. x=constant provides growing F as n increases (22):

$$n\uparrow \rightarrow \downarrow/E_d/ \rightarrow \uparrow F \text{ (if x=constant)} \rightarrow \uparrow /\%RCM(LAN)/$$

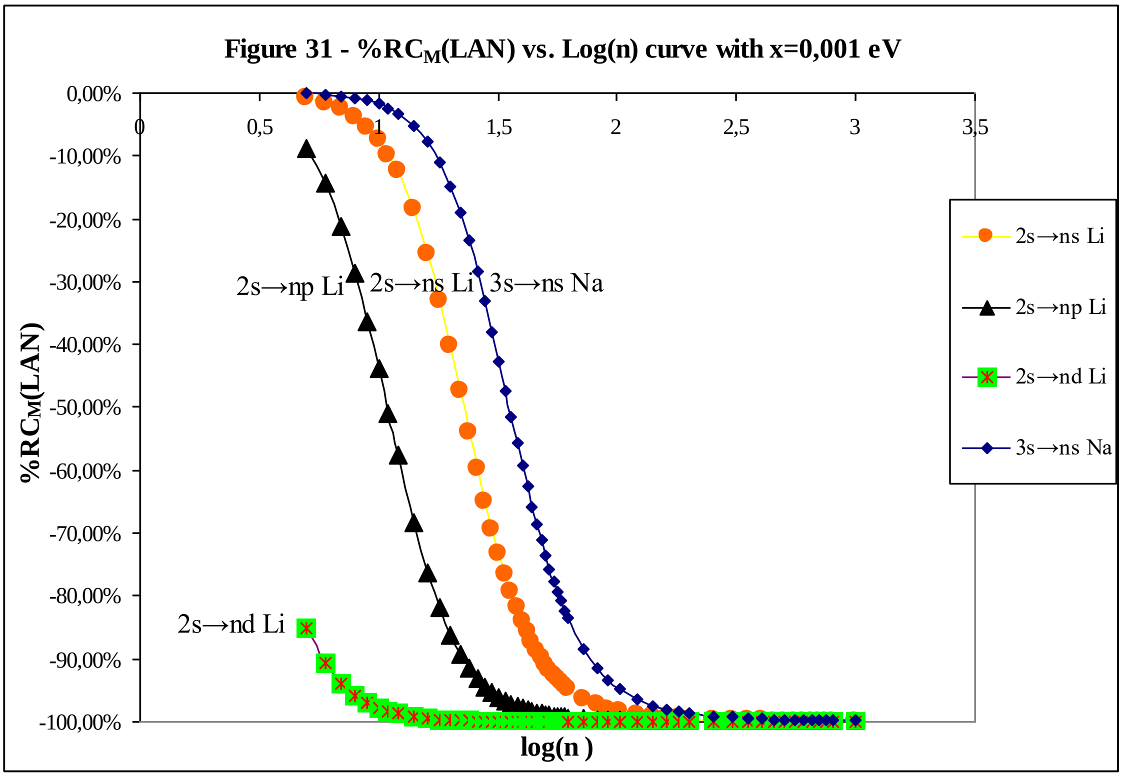

$\%RC_M(LAN)$ has more dramatic variations if situation is reverse: F<1 or x<0. Discontinuity pointed out in c) $\%RC_M(LAN)\rightarrow\pm\infty$ provokes said variability increase. n discontinuity condition applied to F (34) is extended to x (35).

$$(35)\text{n discontinuity condition} = \frac{LAN}{1-F^{1/2}} = \frac{LAN}{1-\left(\frac{E_d+x}{E_d}\right)^2}$$

E_d (36) is obtained from (15) and inserted into (35) to provide (37):

$$(36) E_d = -\left(\frac{K_{LAN}}{n - LAN}\right)^2$$

$$(37) \text{n discontinuity condition} = \frac{LAN}{1 - F^{1/2}} = \frac{LAN}{1 - \left(\frac{-\left(\frac{K_{LAN}}{n - LAN}\right)^2 + x}{-\left(\frac{K_{LAN}}{n - LAN}\right)^2}\right)^2}$$

(37) calculation for jumps with x can be obtained after calculating resulting third degree equation.

Jumps with elevated LAN may appear to have lower $\%RC_M(LAN)$ considering what is seen in Figure 29 and 31, but one element of capital importance is missing: increasing LAN (for same jump and z_s) requires raising n_s and this implies increasing z_o (i.e. atomic number) and its associated ER_o (Excess Relativistic of 1s ionization energy (E_o) in the vision of said 1s ER).

Consequently, Cs I 6s→ns with respect to Na I 3s→ns has two opposite effects:

Positive: ↑LAN → ↓%RCM(LAN)
Negative: ↑Z (or z_o) → ↑/E_o/ → ↑ER_o → ↑%RCM(LAN)

Negative effect wins and, for example in this Cs I 6s→ns, Relation of Riquelme de Gozy without ER_o considerations has much greater curvature than Na I 3s→ns.

G is E_o deviation factor (24) in analogy to F with E_d (6). (24) implies that 1s ionization energy (E_o) is multiplied by factor G to provide E_{oM}. (16) remains as (25) with E_{oM} inclusion:

$$(24) E_{oM} = E_o G$$

$$(25) \%RC_M(LAN) = \frac{1 - \left(\frac{F}{G}\right)^{1/2}}{-1 + \frac{n\left(\frac{F}{G}\right)^{1/2}}{n - LAN}} \bullet 100$$

(8.B) expresses LAN_M with modification in both energies. $\%RC_M(LAN)=0$ when F=G because LAN_M=LAN and can also be seen as (25) is changed to (26)

$$(8.B)\ \text{-}\ LAN_M = \frac{(-E_{oM})^{1/2} z_s}{(-E_{dM})^{1/2} z_o} - n = \frac{(-E_o G)^{1/2} z_s}{(-E_d F)^{1/2} z_o} - n = \frac{(-E_o - y)^{1/2} z_s}{(-E_d - x)^{1/2} z_o} - n$$

$$(26)\%RC_M(LAN)_{F\,=\,G} = \frac{1-1}{-1+\frac{n}{n-LAN}} \bullet 100 = \frac{0}{-1+\frac{n}{n-LAN}} \bullet 100 = 0$$

G and y (27)(28)(29) play the same role as F and x (20)(21)(22):

$$(27)E_{oM} = E_o + y$$

$$(28)E_o G = E_o + y$$

$$(29)G = \frac{E_o + y}{E_o}$$

LAN^* (30) (seen as (28) in article) is specific case in which relativistic effects on LAN are calculated and where x is (31) and y is (32):

$$(30)\ \text{-}\ LAN^* \approx -LAN_R{}^* = \frac{(-E_o{}^*)^{1/2} z_s}{(-E_{dR}{}^*)^{1/2} z_o} - n = \frac{(-E_o - ER_o)^{1/2} z_s}{(-E_{dR} - ER_{dR})^{1/2} z_o} - n$$

$$(31)\ x = ER_{dR}$$

$$(32)\ y = ER_o$$

ARTICLES INDEX		
Part	**Number**	**Title**
Part I - Victoria Equation and Feliz Solutions	01	Victoria Equation - The dark side of the electron.
	02	Electronic extremes: orbital and spin (introduction)
	03	Relations between electronic extremes: Rotation time as probability and Feliz I.
	04	Feliz II the prudent: Probability radial closure with high order variable C_F
	05	Feliz III The King Major: Orbital filled keeping Probability electronic distribution.
	06	Feliz IV Planet Coupling: Probability curves NIN coupling from origin electron.
	07	NIN Coupling values in n=2 and Oxygen electronic density.
	08	Electron Probability with NIN coupling in n=2.
	09	Electron probability with NIN coupling in n>2 and necessary NIN relationships.
Part II – Excited electron: Tete Vic and LAN	10	Excited electrons by Torrebotana Central Line: Tete Vic Equation.
	11	Excited electrons: LAN plains for Tete Vic Equation.
	12	Relation of Riquelme de Gozy: LAN linearity with energy of excited states.
	13	Relation of Fly Piep de Garberí: LAN^{-1} and Ionization Energy.
	14	Relation of Silva de Peral & Alameda: LAN interatomicity with energetic relation.
	15	Relation of Silva de Peral & Alameda II: jump from n_Ss to ns.
	16	SPA III: Mc Flui transform for Silpovgar III and Silpovgar IV.
	17	SPA IV: Silpovgar IV with Piepflui. Excess Relativistic: influence in LAN and SPA
	18	Feliz Theory of Eo vision - Relativistic II: influence in Riquelme de Gozy
	19	Pepliz LAN Empire I: $LAN_{n\to\infty}$ vs. LAN(P50)
	20	Pepliz LAN Empire II: $LAN_{n\to\infty}$ vs. LAN(P50)
Part III - NIN: C_{PEP} & C_{POTI}	21	Electron Probability: PUB C_{PEP} I (Probability Union Between C_{PEP}) - Necessary NIN relationships
	22	Electron Probability: PUB C_{PEP} II in "Flui BAR" (Flui (BES A (Global Advance) Region)
	23	Orbital capacity by advancement of numbers - Electron Probability: PUB C_{PEP} III: "Flui BAR" II and $C_{PEP\text{-}i}$
	24	Electron Probability: 1s electron birth: The last diligence to Poti Rock & Snow Hill Victoria
24 hours of new day		